Fluorescence in air with moisture excited by electrons of 0.85MeV and the effects to the energy determination of ultrahigh-energy cosmic rays

Y.Watanabe[1], M.Nagano[1], K.Ando[2], K.Kobayakawa[3] and N.Sakaki[4]

Abstract

Photon yields in air with moisture excited by an electron using a ^{90}Sr β source are compared with those in dry air. Water vapor considerably reduce the yields, however, effects to the energy determination of ultrahigh-energy cosmic rays are negligible to the measurements at high altitudes like HiRes, TA and Auger sites. Though the effects around the shower maximum may be small for most showers observed from space like JEM-EUSO, the reduction of photon yields due to water vapor must be taken into account to interpret the longitudinal developments of extensive air showers near sea surface (like neutrino induced showers).

1 Introduction

Photon yields in air with moisture are quite important to estimate the primary energy of cosmic rays with the fluorescence technique from space like JEM-EUSO(Japanese Experiment Module - Extreme Universe Space Observatory) [1]. After our previous measurement in dry air [2, 3], the measurement has been continued using ^{90}Sr β source to study the pressure dependence of photon yields for radiation in air with moisture. Preliminary results in 21% to 56% relative humidities around 20°C at one atmosphere are described in Sakaki et al. [4]

2 Photon yield

In the present experiments we measure the number of photons, $\epsilon_i(p)$, per unit length per electron for ith band at pressure p. The fractional energy emitted as photons in total energy loss of an electron in gas, $\varphi_i(p)$, is expressed by

$$\varphi_i(p) = \frac{\epsilon_i(p) h\nu_i}{\rho \frac{\mathrm{d}E}{\mathrm{d}x}} \ , \tag{1}$$

where $h\nu_i$ is the photon energy for the ith band, ρ is the gas density in kg/m^3 and $\frac{\mathrm{d}E}{\mathrm{d}x}$ is the total energy loss of an electron in eV/kg/m^2. We have called $\varphi_i(p)$ as the modified efficiency [4] and is related to the fluorescence efficiency, $\Phi_i(p)$, as

$$\varphi_i(p) = \kappa_i \Phi_i(p) \ .$$

The meaning of a parameter κ_i is described in Sakaki et al.[4].

From the equation of state of a gas, $p = \rho R_g T$ where R_g is the specific gas constant in m^{2}s^{-2}K^{-1} and Eq.(1), $\epsilon_i(p)$ is written as a function of p at a constant temperature T in Kelvin as

$$\epsilon_i(p) = \frac{p}{R_g T} \frac{\mathrm{d}E}{\mathrm{d}x} \left(\frac{1}{h\nu_i} \right) \cdot \varphi_i(p) \ . \tag{2}$$

[1] Department of Space Communication Engineering
[2] Department of Environmental and Biotechnological Frontier Engineering
[3] Faculty of Human Development, Kobe University
[4] Department of Physics and Mathematics, Aoyama Gakuin University

The observed decay time τ of the fluorescence is related to the following three terms: (a) the mean lifetime of the excited state for decay to any lower state, τ_r, with which the fluorescence radiates, (b) that of internal quenching (internal conversion plus inter-system crossing), τ_q and (c) the lifetime of collision de-excitation, τ_c. This can be expressed as follows; (In the following the subscript i for the ith band is omitted in some parts.)

$$\frac{1}{\tau} = \frac{1}{\tau_r} + \frac{1}{\tau_q} + \frac{1}{\tau_c} \equiv \frac{1}{\tau_0} + \frac{1}{\tau_c} , \tag{3}$$

and $\Phi(p) = \frac{\tau}{\tau_r}$. The reciprocal of τ_c is the rate of collision de-excitation and is expressed by

$$\frac{1}{\tau_c} = n\sigma\bar{v}_{rel} = n\sigma\sqrt{\frac{8k_BT}{\pi\mu}} , \tag{4}$$

where n is the number density, σ is the cross-section of collision de-excitation between molecules of mass m_1 and m_2, $\bar{v}_{rel}$ is the average of relative velocities between molecules and μ is the reduced mass of m_1 and m_2. Here we introduce the reference pressure p'. When the pressure $p = p'$, $\tau_0 = \tau_c$, i.e. $\frac{p}{p'} = \frac{\tau_0}{\tau_c}$. Since $p = nk_BT$, where k_B is Boltzmann constant, and if collisions of N_2^* with N_2, O_2 and H_2O are independent with each other, then we have for air with moisture,

$$\frac{1}{p'} = (f_n q_{nn} + f_o q_{no} + f_w q_{nw})\tau_0 . \tag{5}$$

Here f_n, f_o, f_w are fractional pressures (or number densities) of N_2, O_2 and H_2O, respectively and normalized to $f_n + f_o + f_w = 1$. q_{nn}, q_{no} and q_{nw} are the the quenching rate constants for the collision de-excitation and are expressed by

$$q_{12} = \sqrt{\frac{8}{\pi\mu_{12}k_BT}}\sigma_{12} , \tag{6}$$

where 12 stands for nn, no and nw which are collisons of N_2^* with N_2, O_2 and H_2O, respectively. For pure nitrogen gas $f_o = f_w = 0$ and for dry air approximately $f_n = 0.79$ and $f_o = 0.21$.

Using p', Eq.(3), Eq.(2) and Eq.(1) are rewritten in the following;

$$\frac{1}{\tau_i} = \frac{1}{\tau_{i0}}\left(1 + \frac{p}{p_i'}\right) , \tag{7}$$

$$\epsilon_i(p) = \frac{C_i p}{1 + \frac{p}{p_i'}} , \quad \text{and} \tag{8}$$

$$\frac{1}{\varphi_i(p)} = \frac{\eta_i}{C_i}\left(1 + \frac{p}{p_i'}\right) , \tag{9}$$

where

$$C_i = \frac{1}{R_gT}\frac{\mathrm{d}E}{\mathrm{d}x}\left(\frac{1}{h\nu_i}\right)\cdot\kappa_i\Phi_i^\circ \equiv \eta_i\kappa_i\Phi_i^\circ . \tag{10}$$

Φ_i° cooresponds to the fluorescence efficiency in the absence of collision quenching.

3 Air with moisture

The specific humidity (h_s) is defined by the ratio of mass of the water vapor (m_w) to that of air with moisture ($m_w + m_d$), where m_d is the mass of the dry air. If we express the water vapor

Table 1: Experimental conditions (Relative and specific humidities at 1 atm. The average temperatures and their deviations during the run are listed.)

Relative Humidity	Temperature	Specific Humidity	Pressure at enclosure
%	°C	g/kg	hPa
0.0	18.5 ± 1.0	0.0	1013
20.0	20.7 ± 0.7	3.03	1005
35.8	20.7 ± 0.4	5.45	1000
37.8	23.1 ± 1.3	6.65	1003
48.2	20.1 ± 0.59	6.96	1019
48.9	21.0 ± 1.1	7.52	1011
50.0	20.4 ± 0.6	7.46	1004
58.8	20.5 ± 0.5	8.74	1015
64.4	20.60 ± 0.03	9.67	1012

pressure as e (hPa) and the total pressure of air with moisture $p = p_d + e$ (hPa), h_s is written as follows:

$$h_s \equiv \frac{m_w}{m_w + m_d} = \frac{0.622e}{p - 0.378e} = \frac{0.622e_s h_r}{p - 0.378e_s h_r} \ . \tag{11}$$

In this equation, 0.622 comes from the ratio of the molecular weight of water vapor (18.015) to the average molecular weight of real dry air (28.961) and the relation $h_r = e/e_s$ is used, where h_r is the relative humidity and e_s is the saturated vapor pressure at a given temperature (T).

After a simple calculation, we can connect h_s with the fractional pressure f's appeared in Eq.(5) such as,

$$f_n = \frac{0.79 \times 0.622(1 - h_s)}{0.622 + 0.378h_s}, \quad f_o = \frac{0.21 \times 0.622(1 - h_s)}{0.622 + 0.378h_s}, \quad f_w = \frac{h_s}{0.622 + 0.378h_s} \ , \tag{12}$$

where h_s is in g/g.[5]

4 Experiment 1

The experimental details are described in [2, 3]. The central values of the narrow band filters used in the present measurement are 337.7, 356.3 and 392.0 nm and their bandwidths at half maximum are 9.8, 9.3 and 4.35 nm, respectively. (We designate each filter band as 337, 358 and 391 nm hereafter). The measurements have been done in dry air (mixing of 79% nitrogen and 21% oxygen) and in real air with different h_r at one atmosphere by using ^{90}Sr β source of which average energy is 0.85 MeV. The pressure was varied from one atmosphere to 10 hPa under the constant temperature. The experimental conditions are listed in Table 1.

The photon yield ϵ is determined from the number of signal counts, the total number of electrons, the length of the fluorescence portion, the solid angle of the photomultiplier(PMT), the quartz window transmission, the filter transmission and the quantum efficiency and the collection efficiency of the PMT as described in [3]. The $\frac{dE}{dx}$ with E=0.85 MeV is calculated from a formula given in Sternheimer et al. [5].

Here the pressure dependence of ϵ in dry and air with moisture is determined by assuming h_s to be constant, when p is reduced through the thin pipe by the oil-rotary vacuum pump.

[5]Though h_s is dimensionless, hereafter h_s is written in g/kg for numerical values.

Table 2: p' and C values for dry air and eight specific humidities.

	337 nm		358 nm		391 nm	
h_r	p'	$C \times 10^{-3}$	p'	$C \times 10^{-3}$	p'	$C \times 10^{-3}$
%	hPa	1/hPa·m	hPa	1/hPa·m	hPa	1/hPa·m
0.0	22.1± 1.1	48.6 ±4.1	27.1± 3.8	36.5 ±4.5	5.39± 0.82	50.1 ±7.1
20.0	24.2± 1.6	42.4 ±2.4	30.3± 5.2	32.4 ±4.8	8.96± 0.98	30.7 ±2.0
35.8	110.9± 8.2	9.75±0.59	131. ±20.	8.7 ±1.1	56.1 ± 7.8	5.27±0.63
37.8	128.0± 5.6	8.57±0.30	157. ±26.	7.28±0.95	64.1 ± 6.5	4.50±0.40
48.2	110.6± 1.9	9.67±0.48	113. ±17.	9.6 ±1.1	51.2 ± 9.0	5.37±0.80
48.9	99.6± 7.3	10.5 ±0.6	139. ±18.	7.78±0.78	55.2 ± 7.4	5.23±0.59
50.0	124. ±14.	10.8 ±1.2	129. ±20.	8.8 ±1.1	51. ±12.	5.4 ±1.1
58.8	124.0± 7.5	8.41±0.41	176. ±23.	6.42±0.62	62.8 ± 6.9	4.50±0.41
64.4	161.2± 7.7	6.80±0.25	180. ±18.	6.30±0.46	105. ±11.	2.90±0.25

The h_r was not measured at smaller pressure than 1 atm.. The obtained ϵ in each run are fitted to Eq.(8) by iteration with the least square(LS) method and the best fitted p' and C are determined. In these fittings, the contribution of different bands in one filter band width are not separated, which is different from the results in our previous paper [2]. Best fitted p' and C values are listed in Table 2 and p' values are plotted as a function of h_s by dots in Fig. 1. They are extraordinary large at h_s above 5 g/kg.

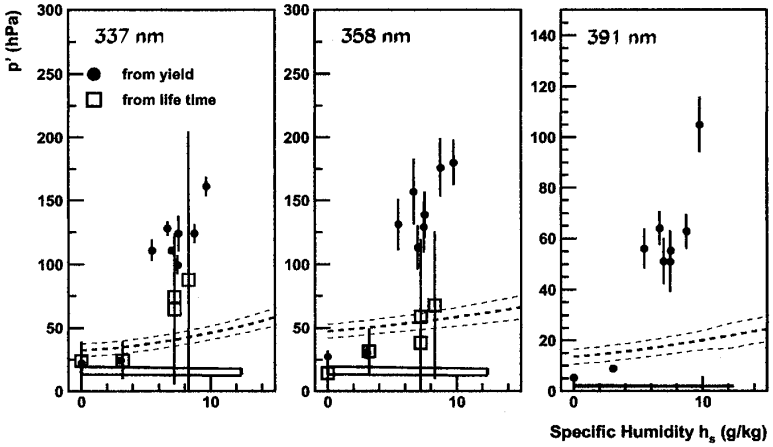

Figure 1: p' values are plotted as a function of specific humidity. Dots are from pressure dependence of ϵ and squares are from pressure dependence of live times. Rectangles and a thin line are expected values from quenching rate constants by using Eq.(5). Heavy dash curves are p' values determined from Experiment 2 (see text) and thin dash ones are their upper and lower bounds.

p' can be determined independently from p dependence of fluorescence lifetime (τ_i) in each band. The reciprocal of measured lifetimes ($1/\tau_i$) at different p's are fitted to Eq.(7). The results are also plotted in Fig. 1 by squares.

By using the measured σ_{nn} and σ_{no} previously reported [3], the quenching rate constants

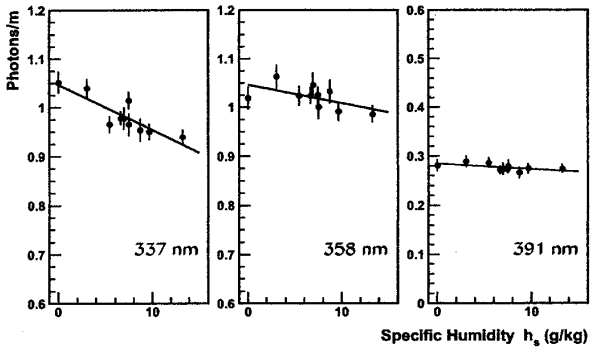

Figure 2: Fluorescence yields at 1 atm. are plotted as a function of specific humidity.

Table 3: Radiative lifetimes and quenching rate constants of q_{nn}, q_{no} and q_{nw}.

Transition	Author	τ_0	q_{nn}	q_{no}	q_{nw}
		ns	$\times 10^{-4}$hPa^{-1}ns^{-1}		
	Nagano et al.[3]	30.0±1.7	2.46±0.15	64.5± 4.6	
337 nm	Brunet [7]	31. ±6.	2.83±0.14	67.5± 9.0	102. ±27
2P(0,0)	Morozov et al.[8]	41.7±1.4	2.97±0.25		175. ±18
	Pancheshnyi et al.[9]	42. ±2.	3.21±0.49	74.2± 7.4	96.4± 9.9
	Colin [10]	37.	2.5	62	100
	Nagano et al.[3]	32.2±0.5	2.80±0.11	60.8± 4.9	
358 nm	Brunet [7]	36. ±8.	6.76±0.30	75. ±13.	102. ±27
2P(1,0)	Morozov et al.[8]	41.7±2.1	6.2 ±0.2		165. ±17
	Pancheshnyi et al.[9]	41. ±3.	7.2 ±0.7	76. ± 7	91. ±10
	Colin [10]	38	6.5	80	95
391 nm	Pancheshnyi et al.[9]	62. ±6	52. ±5	126. ±12	213. ±22
1N(0,0)	Colin [10]	65.	65	150	200

of q_{nn} and q_{no} are calculated at 20°C from Eq.(6). They are listed in Table 3 together with the results by H.Brunet[7], A.Morozov et al.[8], S.V.Pancheshnyi et al.[9] and P.Colin[10]. Since $q_{nw} > q_{no} > q_{nn}$, $\frac{1}{p'}$ increases with f_w increases as is seen from Eq.(5). p' estimated with values in Table 3 are within rectangles for 337 nm and 358 nm and a thin line for 391 nm in Fig. 1. p' decreases with h_s slightly and much smaller than the experimental values, especially above h_s=5 g/kg. Their large differences may be due to the assumption that h_s doesn't change with p when p is reduced through the narrow pipe by the vaccum pump. That is, h_s at reduced p than 1 atm. may not be reliable. Therefore ϵ only at 1 atm. are plotted in Fig. 2 as a function of h_s. Since the errors are large, they are fitted to a linear function and are drawn by heavy lines.

5 Experiment 2

According to the vacuum technique[11], considerable time t_w is required for the flow to be steady when the reduction or inclusion of air with moisture is made through a narrow pipe. The time required depends on the length of the pipe L, inner radius r, velocity of water molecules v,

smoothness of the surface β, attachment probability a, and the average attachment time t_a and is expressed by

$$t_w \sim \frac{1}{4}\left(\frac{L}{r}\right)^2\left(\frac{2r}{v}+\beta a t_a\right) \sim \frac{1}{4}\left(\frac{L}{r}\right)^2 \beta a t_a \ . \tag{13}$$

Putting r=3.3 mm, L=34 cm and β=1, $t_w = 664 a t_a$. If we assume a=1, t_a is an order of 1 minute, then t_w is an order of 1 day. Since we change pressure within an order of 10 minutes, the change of partial pressure of water vapor may be not proportional to the change of total pressure so that h_s changes with p. In the following we use at any pressure h_r measured with VAISALA HMP234(Y2330008), which was calibrated at 1 atm. with the newly calibrated VAISALA HMP234-06 at the VAISALA factory. The humidity sensor is a capacitive thin-film polymer whose dielectric properties depend on the amount of water contained in it.

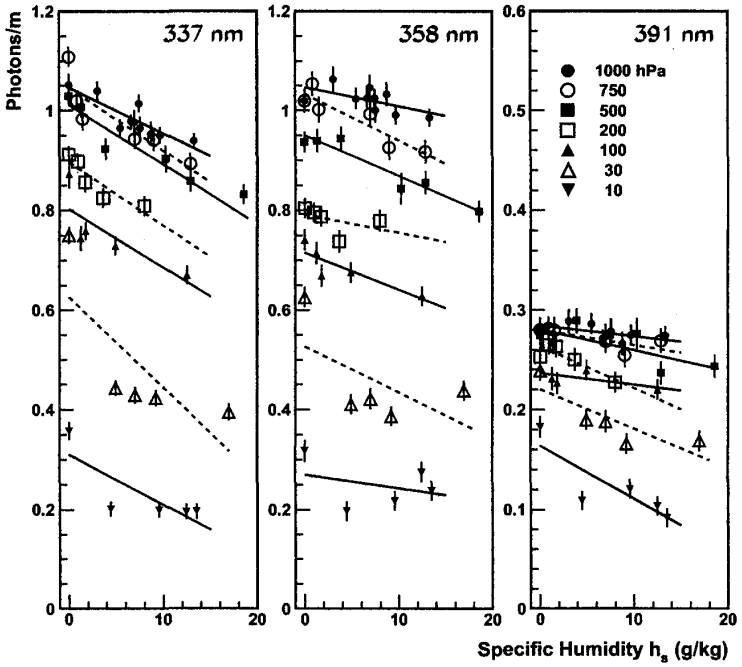

Figure 3: Fluorescence yields at 1000, 750, 500, 200, 100, 30 and 10 hPa are plotted as a function of specific humidity.

Measurements have been made at 1000, 750, 500, 200, 100, 30 and 10 hPa at different h_r. Each run took about 1 week and the average h_r and T, which were recorded each 30 sec, during the run are used to convert them to h_s by using Eq.(11). Fluorescence yields at seven pressures thus determined are plotted as a function of h_s in Fig. 3. Solid and dashed lines are the linear fits at each pressure. Errors are statistical only and seem that the systematic ones are much larger than the statistical ones.

By using linear fitted lines, we have determined ϵ at constant h_s and p. Then p' have been determined by fitting the obtained ϵ to Eq.(8). The results are drawn by heavy dash curves in Fig. 1. Thin dash ones are their 1σ errors. p' are closer to the estimated one from quenching rate constant, however, there remain still large discrepancies.

6 Effects of the present results to the energy estimation of extensive air showers

In the present measurement the temperature was kept constant for decreasing the pressure. Actually, the atmospheric temperature decreases with the lapse-rate of about 6.5 K/km. In the left panel of Fig. 4, average h_s is plotted as a function of altitude at latitudes 30°N and 45°N in January and June. h_s are calculated from T and h_r using Eq.(11). Average of annual values at 15°N are also shown [12]. h_s is less than 3 g/kg above 5 km, irrespective of seasons.

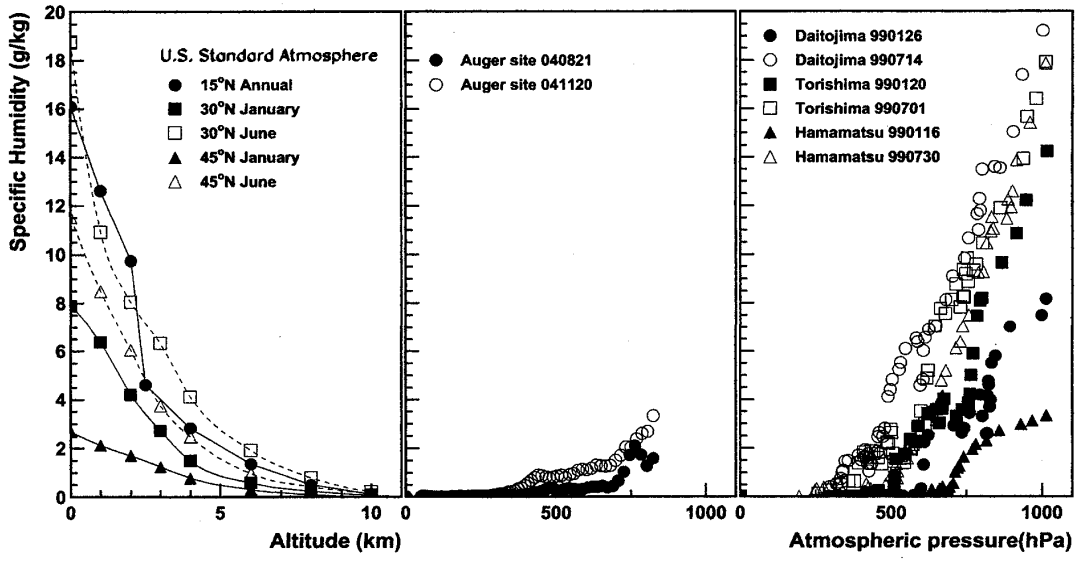

Figure 4: In the left panel, average h_s is plotted as a function of altitude at latitudes 30°N and 45°N in January and June. Average of annual values at 15°N are also shown. In the central one, h_s are plotted as a function of atmospheric pressure at Auger site [13] and in the right panel at Minamidaitojima, Minamitorishima and Hamamatsu [14] in summer and winter. Numbers listed mean the date of measurements. For example, 040821 stands for 21st of August, 2004.

In the central one, h_s are plotted as a function of atmospheric pressure in Auger experimental site [13] and in the right panel are plotted those at Minamidaitojima and Minamitorishima as examples over the Pacific ocean [14]. h_s is less than 3 g/kg at Auger site throughout a year. In case of the Pacific ocean h_s may be less than 5 g/kg above 500 hPa throughout a year, however, it becomes quite high even in winter near sea level.

Ratios of $\epsilon(h_s)$ at h_s to that for dry air are drawn by a heavy line for p=1000 hPa, a heavy dashed line for 750 hPa and a heavy dash-dot line for 500 hPa in Fig. 5. Thin lines are upper and lower 1σ bounds for each p. If h_s is less than 3 g/kg at Auger site, the decrease of photon yields may be less than 5% throughout a year, as far as the data provided are typical at Auger site. In case of JEM-EUSO, we need detailed simulation to evaluate the effects quantitatively. Especially the decrease of photon yields due to water vapor near sea surface (for neutrino shower) can't be ignored.

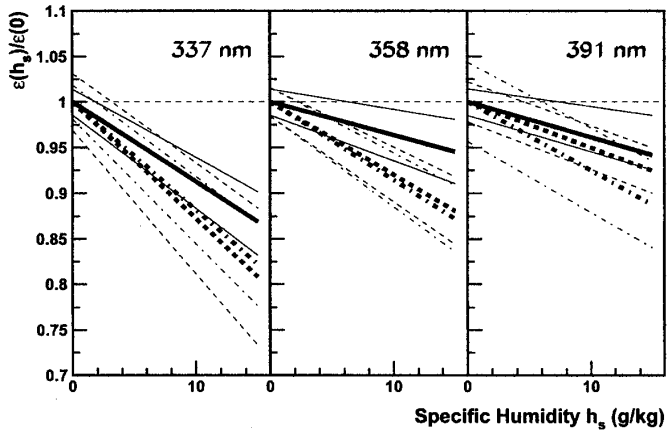

Figure 5: Ratios of $\epsilon(h_s)$ at h_s to that at h_s=0 are drawn by a heavy line for p=1000 hPa, a heavy dashed line for 750 hPa and a heavy dash-dot line for 500 hPa. Thin lines are upper and lower 1σ lines for each p.

7 Conclusion

Photon yields in air with moisture were investigated and compared with those in dry air. Though the rate of the mole number of water to the total mole number is small in air with moisture, the effect to the yields near sea surface can't be ignored. There are some discrepancy in p' between experiment and those expected from Eq.(5) as shown in Fig. 1. For quantitative evaluation of the effects to the yields and the interpretation of the fluorescence properties of air with moisture, we need further refinements of the experiments.

This work is supported in part by the grant-in-aid for scientific research No.15540290 from Japan Society for the Promotion of Science and in part by the FUT Research Promotion Fund.

References

[1] T. Ebisuzaki et al., "JEM-EUSO mission to attach JEM/EF of ISS", (2006).

[2] M. Nagano, K. Kobayakawa, N. Sakaki and K. Ando, Astropart. Phys. **22**, 235 (2004).

[3] M. Nagano, K. Kobayakawa, N. Sakaki and K. Ando, Astropart. Phys. **20**, 293 (2003).

[4] N. Sakaki, K. Kobayakawa, M. Nagano, Y. Watanabe and K. Ando, Proc. 29th Int. Cosmic Ray Conf. (Pune, India), **v.7** (2005) 185.

[5] R.M. Sternheimer et al., Phys. Rev. **B26** (1982) 6067.

[6] F.R. Gilmore et al., J. Phys. Chem. Data 21, 1005 (1992).

[7] H. Brunet, PhD. Thesis, A L'université Paul-Sabatier de Toulouse (1973)

[8] A. Morozov et al., Euro. Phys. J., **33** (2005) 207.

[9] S.V. Pancheshnyi et al., Chem. Phys., **262** (2000) 349.

[10] P. Colin, PhD. Thesis, Laboratoire d'Annecy de Physique des Particlules - 1N2P3 (2005).

[11] "Shinkugijyutu" (ed. by C. Hayashi, Kyoritsu Shuppan Ltd.) (1985)

[12] "US Standard Atmosphere 1976", U.S. Government Printing Office, Washington D.C. (1976).

[13] B. Keilhauer, private communication (2004)

[14] Radiosonde data by Japan Meteorological Agency (1999)

(Received March 22. 2007)